Precipitation Structures of a Thermal Convective System Happened in the Central Western Subtropical Pacific Anticyclone[*]

Fu Yunfei[1,2](傅云飞), Feng Jingyi[3](冯静夷), Zhu Hongfang[4](朱红芳), Li Rui[2](李 锐), and Liu Dong[2](刘 栋)

1 *Institute of Heavy Rain, CMA, Wuhan* 430074

2 *School of Earth and Space Sciences University of Science and Technology of China, Hefei* 230026

3 *Office of Weather Modification in Anhui, Hefei* 230026

4 *Weather Observatory Station in Anhui, Hefei* 230026

ABSTRACT

In this paper, characteristics of precipitating clouds in a thermal convective system (TCS) occurred in the southeastern mainland of China at 15:00 BT (Beijing time) on August 2, 2003 in the central western subtropical Pacific anticyclone (WSPA) is studied by using TRMM tropical rainfallmeasuring mission PR (precipitution radar) and IR Infrared radiation measurements. The precipitating cloud structures in both horizontal and vertical, relationship among storm top, cloud top, and surface rain rate are particularly analyzed. Results show that a strong ascending air at 500 hPa and a strong convergence of moisture flux at 850 hPa in the central WSPA supply necessary conditions both in dynamics and moisture for the happening of the TCS precipitation. The TRMM PR observation shows that the horizontal scale of the most TCS precipitating clouds is about 30-40 km, their averaged vertical scale is above 10 km, and the maximum reaches 17.5 km. The maximum rain rate near surface of those TCS clouds is beyond 50 mm h^{-1}. The mean rain profile of the TCS clouds shows that its maximum rain rate at 5 km altitude is 1 km lower than the estimated freezing level of the environment. Compared with the mesoscale convective system (MCS) of "98.7.20", both systems have the same altitude of the maximum rain rate displayed from both mean rain profiles, but the TCS is much deeper than the MCS. From the altitude of the maximum rain rate to near surface, profiles show that rain rate reducing in the TCS is faster than that in the MCS, which implies a strong droplet evaporation process occurring in the TCS. Relationship among cloud top, storm top, and surface rain rate analysis indicates a large variation of cloud top when storm top is lower. On the contrary, the higher the storm top, the more consistent both cloud top and storm top. And, the larger the surface rain rate, the higher and more consistent for both cloud top and storm top. At the end, results expose that area fractions of non-precipitating clouds and clear sky are 86% and 2%, respectively. The area fraction of precipitating clouds is only about 1/8 that of non-precipitating clouds.

Key words: thermal convective system (TCS), subtropical anticyclone, TRMM PR and IR

1. Introduction

Among atmospheric circulations in summer, the western subtropical Pacific anticyclone (WSPA) zone is a main system determining weather and climate in the most part of China. The variations of the WSPA position together with southwesterly moisture monsoon flow in the lower atmosphere orient the spacial and temporal distribution of rainfall patterns (or named as rainfall band) in China (Tao and Zhu, 1964; Guo, 1985; Zhao and Zhang, 1996; Zhang and Tao, 1998). Because of the closely relationship between

the WSPA and drought/waterlog in the mainland of China, the WSPA has been dramatically studied by Chinese scholars from different aspects (Huang and Li, 1988; Yu and Zhao, 1993; Lu et al., 1995; Wang and Wu, 1997; Liu et al., 1999; Liu and Wu, 2000). Wu et al. (2002) systematically explored and expatiated dynamics of the WSPA formation and its variation mechanism, and exposed characteristics of the WSPA by investigations from data analysis, numerical simulations, and theoretical studies. On the other hand, Tao et al. (1979, 1980) has focused on heavy rain cases in China, and revealed many preconditions for strong

convective development, such as mesoscale convective system (MCS), in large scale atmospheric circulation, weather situation, physical parameters, and so on. Ding (1993) also pointed out that the relationship of air fluid matching between the lower and higher level is very important in the initial and development processes of heavy storms. Recently, results derived from the Huanan and Taiwan Area Mesoscale Meteorological Experiment (HUAMEX) and the Huaihe River Basin Energy and Water Cycle Experiment (HUBEX) indicated a significant dynamical role of topographical forcing on heavy rainfall (Sun et al., 2002; Cui et al., 2002). However, the knowledge of precipitating clouds in the thermal convective system (TCS) inside the central WSPA is limited due to their strong localization, and rough, ineffective routine observations for such kind of cloud.

The Tropical Rainfall Measuring Mission (TRMM) is a joint mission between NASA and the Japan Aerospace Exploration Agency (JAXA) designed to monitor and study tropical rainfall (Simpson et al., 1988). The TRMM satellite onboard the first precipitation radar (PR) together with other instruments was launched in late 1997. Observations of TRMM continuously collected covering the entire tropical belt between 38°S and 38°N provide us a unique opportunity to examine the characteristics precipitating clouds. Using rain profile data derived from PR measurements, the first author and his cooperators have uncovered natures of the horizontal distributions and vertical structures of precipitations (Fu and Liu, 2001, 2003; Liu and Fu, 2001; Fu et al., 2002, 2003a,b, 2004; Li et al., 2005; Zheng et al., 2004). The goal of this paper tries to loosen secrets of precipitating clouds in the TCS inside the central WSPA by analyzing a case happened in South China on August 2, 2003 as viewed by TRMM, which could be helpful for understanding natures of both the TCS and the WSPA.

2. Data

The data used in this paper are standard TRMM products derived from measurements of TRMM PR and VIRS (Visible/Infrared Scanner). TRMM is a non-synchronous satellite with inclination angle 35° approximately. Its orbital altitude is 350 km (regulated to 400 km after August 7, 2001) (Kummerow, 1998). Its earth-circling time is around 96 minutes and there are about 16 orbits between 38°S and 38°N each day. The scanning width of PR is about 220 km. One of standard TRMM products, 2A25, supplies three dimensional rainfall rate from earth surface to 20 km altitude with the horizontal resolution 4.3 km (at nadir) and the vertical resolution 0.25 km, which is retrieved from PR measures (Iguchi and Meneghini, 1994). According to TRMM V algorithm (Awaka et al., 1998), 2A25 contains rainfall type information: convective rains, stratiform rains and others (Fu et al., 2003b; kummerow et al., 1998).

Another standard TRMM product, 1B01, offers the reflectivity of visible light and the infrared radiative (IR) temperature. Both are obtained from the calibrated observations of the TRMM VIRS. The VIRS has 5 channels, i.e., 0.63, 1.60, 3.75, 10.80, and 12.00 μm. The scanning width of VIRS is about 770 km (shifted to 833 km after August 7, 2001), which generates the horizontal resolution 2.2 km (spread out into 2.4 km after August 7, 2001) at nadir. Generally, the lower the radiative temperature radiated from cloud top received by IR, the higher the cloud top. Usually, clouds with higher top are closely allied with convective precipitating clouds except cirrus which has higher cloud top and lower IR temperature but no rainfall output.

In order to get more detailed information of precipitating clouds, a uniform horizontal resolution, PR resolution 4.3 km (at nadir), for both TRMM PR and VIRS must be collocated by unifying both different resolutions. Here, we disregard the observation time difference of both sensors focusing on the same target although there is nearly a minute non-synchronization for them. IR temperature at each uniform horizontal resolution is obtained by weighting average IR temperatures of VIRS pixels located within the PR pixel resolution. After the horizontal resolution unification, each rain profile endues with IR temperature radiated from the precipitating cloud top.
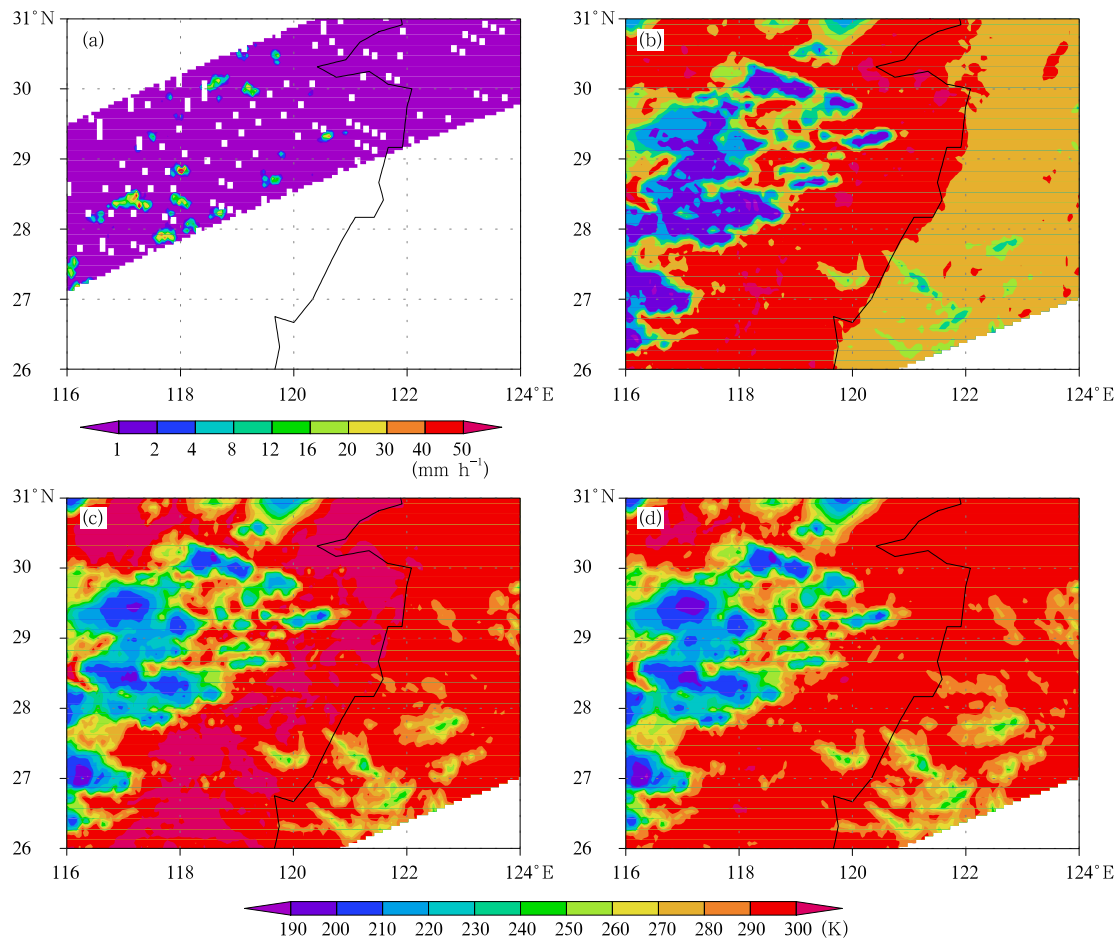
To examine the stability in stratified atmosphere

and atmospheric circulation background, sounding temperatures at 00:00 UT or 08:00 BT at four weather stations (Changsha, Ganzhou, Chenzhou, and Nanchang) in South China and the NCEP/NCAR (National Centers for Environmental Predication/National Center for Atmospheric Research) reanalysis data <http://www.ncep.noaa.gov> are used in the paper.

3. Results

The rain case occurred in South China on August 2, 2003. Figure 1 shows the distributions of near surface rain rate and IR temperatures at 15:41:29 BT at 28.4355°N, 117.155°E as viewed by TRMM PR, IR channels 3.75, 10.80, and 12.04 μm. The isolated precipitating clouds detected by TRMM PR distribute within a space 27°-31°N, 116°-121°E. Although the horizontal scales of these precipitating clouds are smaller than 100 km (see Fig.1a), heavy rain rates are observed near surface for some clouds, the maximum rain rate is greater than 50 mm h^{-1}. On the other hand, several big blocks of clouds appear from the distribution of the lower IR temperatures over the precipitating clouds. If the horizontal scales of these clouds are estimated by IR temperature lower than 260 K, they are between 100 and 200 km (see Figs.1b, 1c, and 1d). It is obvious that the covers of precipitating clouds are only small part within cloud blocks. But locations of precipitating clouds are still judged by the distributions of IR temperatures lower than 210 K approximately. Therefore, in view of precipitating cloud size, the rain case should be defined as meso-β-scale convective system (MCS-β).

Fig.1. Near surface rain rate detected by TRMM PR at 15:41 BT on Aug. 2, 2003 (a), radiative temperature from cloud top measured by IR at channels of 3.75 μm (b), 10.80 μm (c), and 12.00 μm (d).
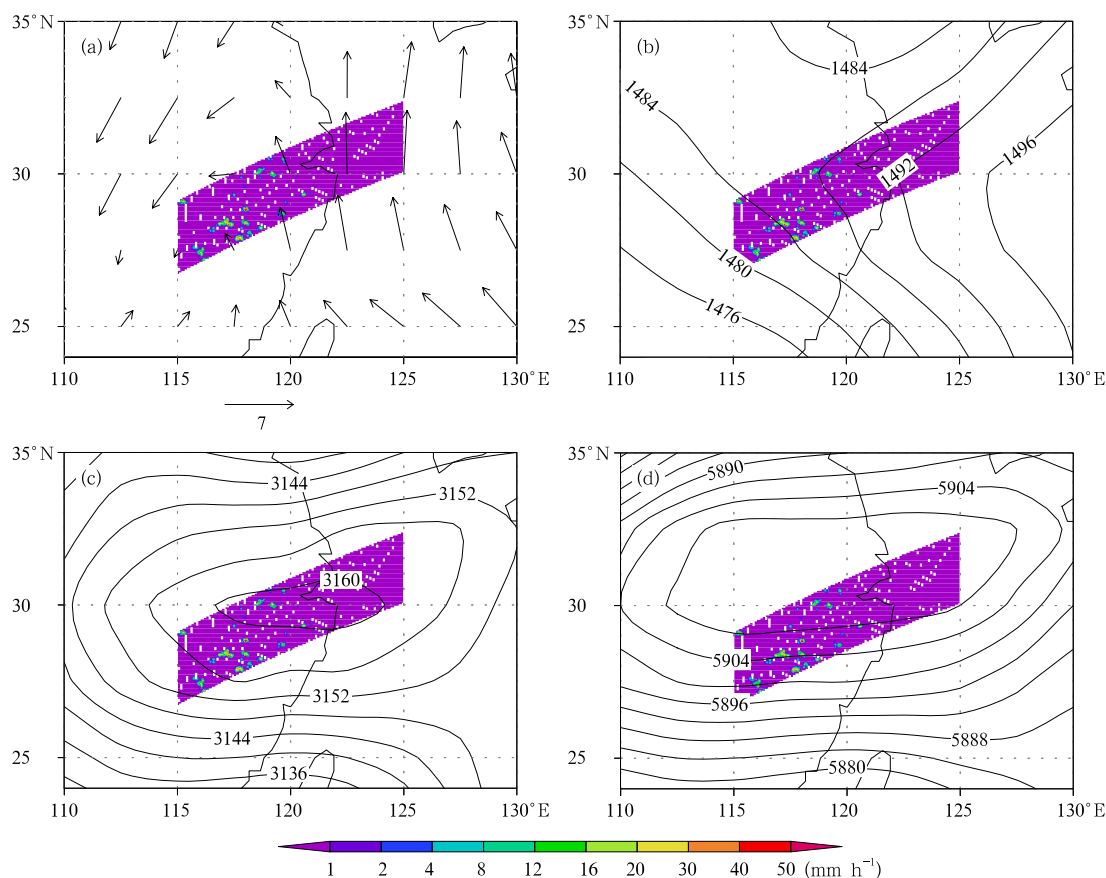
3.1 *Atmospheric background*

To understand atmospheric circulation background for the MCS-β, Fig.2 shows daily averaged wind field at 1000 hPa, geopotential height at 850, 700, and 500 hPa in East China including East China Sea (24°-35°N, 110°-130°E) by using NCEP/NCAR reanalysis daily data overlapped with distributions of rain rate at 2 km detected by TRMM PR. It clearly indicates these isolated precipitating clouds situate within the convergent depression region in the lower atmosphere. At 850 hPa, these precipitating clouds are located inside saddle region. However, at 700 and 500 hPa, the central WSPA is over the head of these precipitating clouds.

To identify the property of the MCS-β, we checked weather records on that day in South China. The records on the surface chart at 14:00 BT display that the maximum temperature is over 39°C, even ex-

ceeding 40°C, observed by most weather stations. On the contrary, the dew-point temperatures at these stations are lower than 26°C, which denotes relatively dry air near surface at that moment in the afternoon. The surface chart also shows weak wind field near surface and non-precipitation happened in South China before 14:00 BT. Now, we deduce that the MCS-β is also a meso-β-scale thermal convective system (TCS) that usually occurs in South China summer although its natures have not been reported officially.

Our deduction has been conformed by tracing per 3-h record in weather diary on that day at three weather stations (Guixi, Jingdezhen, and Guangchang). The records of temperature, dew-point temperature, and weather phenomenon (see Table 1) show clear sky at the two stations before 11:00 BT while miss records at Guixi. At 14:00 BT, temperature beyond 39.9°C is reported at the three stations where clear sky or cloudy sky appears. After 3 h,

Fig.2. Rain rate at 2 km detected by TRMM PR at 15:41 BT on Aug. 2, 2003 and overlapped with daily averaged wind field at 1000 hPa (a), geopotential height at 850 hPa (b), 700 hPa (c), and 500 hPa (d).

Table 1. Records of temperature(Temp.), dew-point temperature (Dew.), and weather phenomenon (Wea.) at three observatory stations on Aug. 2, 2003

	Guixi (58626)			Jingdezhen (58527)			Guangchang (58813)		
	Temp. ($^{\circ}$C)	Dew. ($^{\circ}$C)	Wea.	Temp. ($^{\circ}$C)	Dew. ($^{\circ}$C)	Wea.	Temp. ($^{\circ}$C)	Dew. ($^{\circ}$C)	Wea.
11 BT				37.5	26.0	clear	36.8	22.9	clear
14 BT	40.3	24.9	clear	39.9	23.2	clear	40.3	22.7	cloudy
17 BT	27.5	23.5	light storm	36.0	25.2	dry storm	26.8	24.8	light storm
20 BT	28.4	25.6	cloudy	31.9	20.8	overcast	27.1	24.8	overcast

lightning storm appears at both Guixi and Guangchang while dry lightning storm occurs at Jingdezhen. At 20:00 BT, the lightning storm phenomenon is replaced by overcast sky or cloudy sky at the three stations and air temperature also drops to below 30°C, which means the end of the TCS process.

In order to understand moisture distributions of the TCS in the dry and hot background in the lower atmosphere, the profiles of air temperature, dew-point temperature, and parcel state at 8:00 BT at another four weather stations (Changsha, Ganzhou, Chenzhou, and Nanchang) near the region occurred the TCS precipitation are plotted in Fig.3. Besides, the differences of potential pseudo-equivalent temperature between 700, 500. and 850 hPa are calculated to comprehend atmospheric instability. The configuration of stratification curve together with parcel state profile indicates no instable energy deposited in the atmosphere at 8:00 BT. Furthermore, dry air environment below 500 hPa can be concluded because of relative large gap between air temperature and dew-point temperature at each same level except for Nanchang Station where lower cloud may exist possibly due to the small gap at 850 hPa. The calculated differences of potential pseudo-equivalent temperature show that $\Delta\theta_{se(500-850)}$ values are around -25 K, and $\Delta\theta_{se(700-850)}$ varies from -11 to -20 K, which expresses relatively convective instability state in atmosphere at that moment.
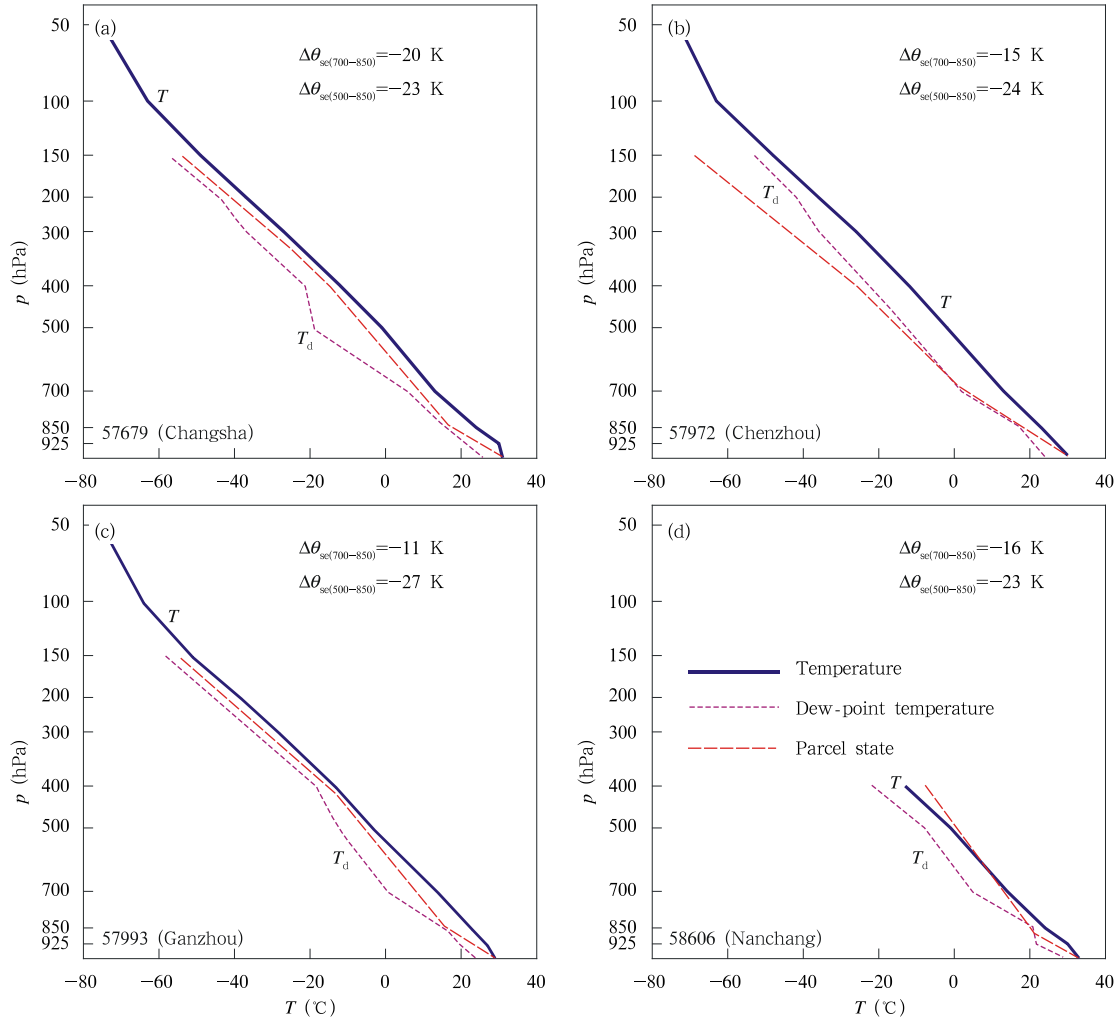
Figure 3 describes atmospheric state near the region of the TCS before 6 h of its occurrence due to shortage of intensively spacial and temporal observation data. As a supplement, the 6-h reanalysis data supplied by the NCEP/NCAR are used to display divergences of moisture flux at 850 hPa overlapped with

vertical velocity (ω) at 500-hPa at 8:00 BT and 14:00 BT in Fig.4. In Fig.4a, it indicates weak descending flows at 500-hPa level suffusing within the region of the TCS in the morning 8 o'clock before the TCS occurs. Only in the south and southwest near the TCS precipitation region there exists a convergent center of moisture flux (-0.75$\times10^{-7}$ cm^2 hPa^{-1} s^{-1}). But 6 h later (i.e., 14:00 BT) in the moment before the TCS precipitation occurrence, strong ascending flows, the maximum reaching -3$\times10^{-3}$ hPa s^{-1}, at 500-hPa level occupy over the TCS region that is located in the northwest of the convergent center of moisture flux at 850 hPa. It is obviously strengthening for that convergent center (value over -1.0$\times10^{-7}$ cm^2 hPa^{-1} s^{-1}) comparing with that in the last 6 hours.
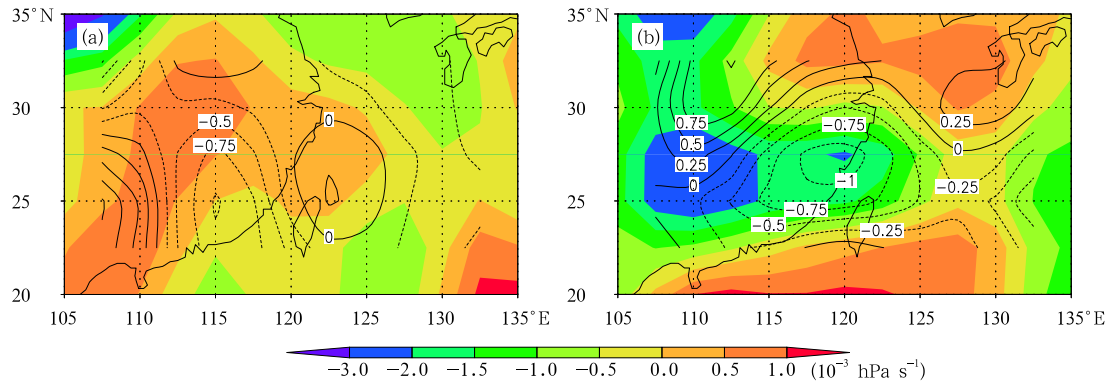
Although Fig.4 derived from the NCEP/NCAR 6-h reanalysis data describes effectively moisture and ascending/descending flow for large scale atmosphere and represents badly thermo-dynamic structures for such meso-β-scale TCS, it may (chosen "may" due to this a case study in this paper) still be used to illustrate the following facts: (1) There is a strong diurnal variability for ascending/descending flow, atmospheric moisture, and stratification state in South China summer in the central WSPA so that limited forecast ability for such kind of TCS happened in the afternoon based on the sounding data at 8:00 BT, actually blurry signs for strong convection in Fig.3; (2) The moist source needed for the TCS development is supplied by convergences of moisture flux at 850 hPa; and (3) Strong ascending air flows can occur in the central WSPA in South China summer due to sun radiative heating forcing, which supplies dynamic forcing condition for local TCS precipitations. In order to get more detailed natures of

such meso-β-scale TCS in both thermo-dynamics and microphysics, conveniently mobile active observation systems such as vehicle onboard precipitation radar are needed urgently in China.

Fig.3. Profiles of temperature, dew-point temperature, and parcel state at four observatory stations at 8:00 BT on Aug. 2, 2003. The number at up right of each panel is $\Delta\theta_{se(700-850)}$ and $\Delta\theta_{se(500-850)}$.

Fig.4. Divergences of moisture flux at 850 hPa overlapped with vertical velocity (ω) at 500 hPa at 8:00 BT (a) and 14:00 BT (b).

3.2 Horizontal scales of the TCS precipitating clouds

Concerning the horizontal scale of the local TCS precipitating clouds, it is uncommonly reported due to their small size and scattering distribution, which results in difficulty to capture them by ground based radars. This shortage of the ground based radars can be retrieved by the TRMM PR. Figure 5 shows convective precipitating pixels at 2-km altitude detected by TRMM PR. Although the sizes of these precipitating clouds marked from A to H vary from 10 km to 80 km, most of their sizes (such as B, C, D, F, and G) are from 30 to 40 km, i.e., meso-β-scale TCS precipitating clouds. Table 2 lists the horizontal scale (l), vertical scale (h), average rain rate at 2 km, and average vertical velocity estimated by average rain rate for the

eight TCS precipitating clouds. The maximum and minimum averaged horizontal scale are 65 km and 10 km, respectively, corresponding to averaged rain rate 13.1 and 5.1 mm h^{-1} at 2-km altitude, respectively. For the most TCS precipitating clouds, their rain rates at 2 km are near or greater than 10 mm h^{-1} except block G and H. They are part of heavy precipitating clouds. The maximum averaged vertical velocity estimated from averaged rain rate is about -8.2$\times10^{-3}$ and -3.2$\times10^{-3}$ hPa s^{-1} for the minimum. Both are greater than the vertical velocity (-3$\times10^{-3}$ hPa s^{-1}) at 14:00 BT in the central ascending region calculated by NCEP/NCAR data. Consequently, it illuminates that NCEP/NCAR reanalysis data is invalid to explain features internal meso-β-scale TCS although the data is effective to describe large scale atmospheric circulation.
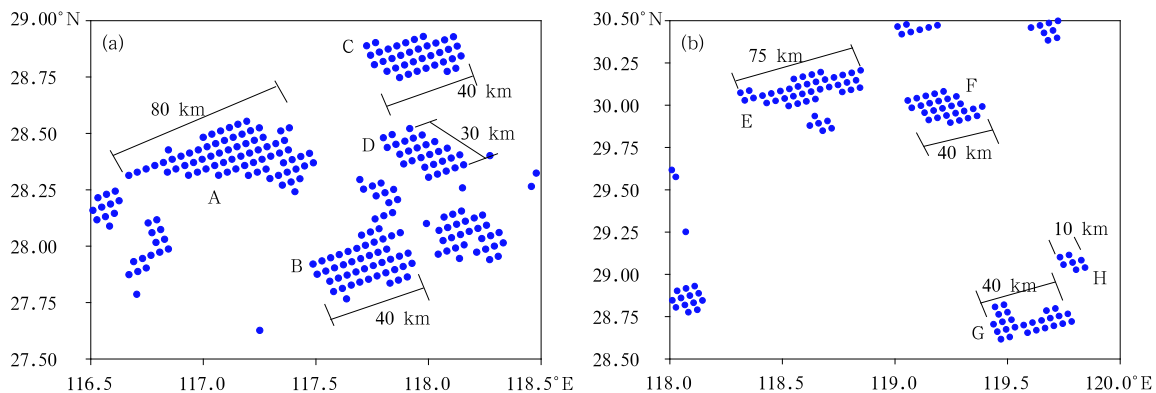
Table 2. Scales in both horizontal (h) and vertical (l), rain rate at 2 km, IR temperature from cloud top, and vertical velocity averaged in each precipitating cloud marked from A to H

	A	B	C	D	E	F	G	H
l (km)	65.0	31.0	31.0	30.0	45.0	32.5	27.5	10
h (km)	17.0	14.0	14.5	17.0	17.75	12.5	10.0	10.5
$\overline{R}$ (mm h^{-1})	13.1	11.8	12.1	11.0	9.4	12.5	8.6	5.1
TB$_{3.75\mu m}$	257.5	261.7	259.1	253.9	255.0	260.9	275.9	285.7
TB$_{10.8\mu m}$	204.4	234.5	230.8	209.1	210.5	229.9	262.6	270.2
TB$_{12.0\mu m}$	202.5	233.4	229.3	207.8	208.7	228.5	261.8	268.2
$\overline{\omega}$ (10^{-3}hPa s^{-1})	-8.2	-7.4	-7.5	-6.9	-5.9	-7.8	-5.4	-3.2

3.3 Vertical structures of the TCS precipitating clouds

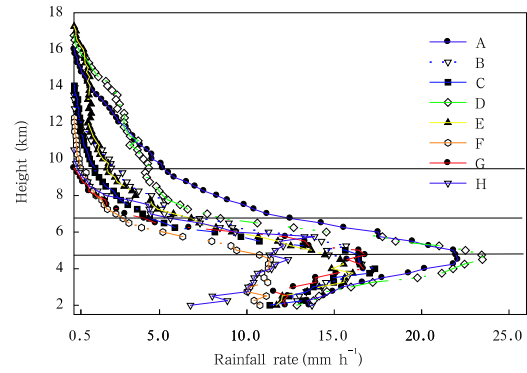The characteristics of thermodynamics and microphysics inside precipitating clouds can be reflected

by the structure of precipitating clouds (Houze, 1997; Tao et al., 1993). Rain profiles are very useful to present these characteristics. When the profile vertically extends up to higher (lower) atmosphere, it suggests strong (weak) ascending flow inside the

Fig.5. Distributions of precipitating pixels of each precipitating cloud marked from A to D (a) and from E to H (b) at 2-km altitude detected by TRMM PR.

precipitating cloud to some extent. On the other hand, the increase (decrease) of rain rate along profile via height (i.e., the various slope of the profile) means more (less) latent heat released by precipitations. Fu et al. (2003a, b) found that the depth of coagulation layer, mixture layer, and droplet broken layer (or evaporation layer sometimes) near surface inside deep convective precipitating clouds in different regions can be characterized by the varied rain rate of profiles, which illustrates different thermo-dynamics and microphysics of precipitating clouds in these regions.
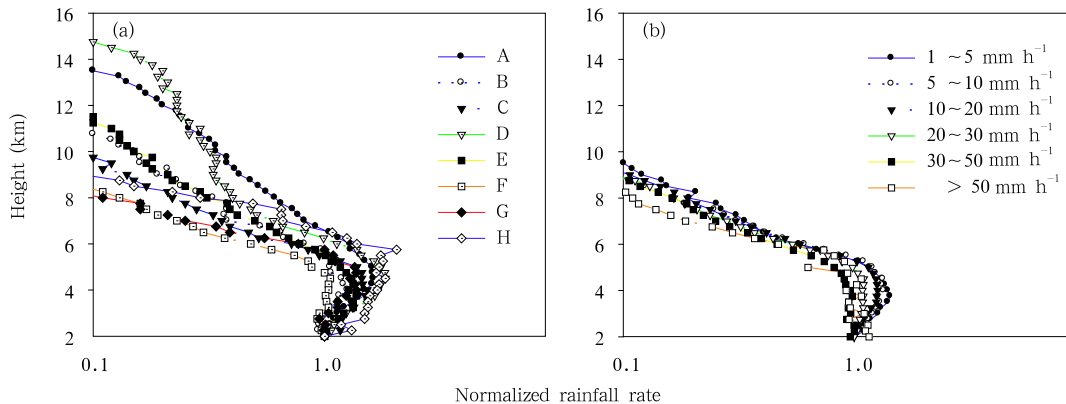
The vertical scale of the eight precipitating clouds shown in Table 2 notifies that these meso-β-scale TCS precipitating clouds are deep convective precipitating clouds. Their mean profiles are plotted in Fig.6, which clearly denotes the maximum averaged rain rate at about 5-km altitude. The altitude is 1 km less than the environmental freezing level height (FLH) estimated from surface temperature $40°C$ with the climatological lapse rate of temperature $6.5°C \ km^{-1}$. However, the actual FLH may vary because of mixing effects caused by vertical flow inside convective clouds. Rain rate drops off rapidly in the layer from the FLH to 7 km, which represents features in the mixture layer of liquid droplets with ice particle droplets as our previous results (Liu and Fu, 2001; Fu and Liu, 2003; Fu et al., 2003a, b). Above the mixture layer to the storm top, slowly dropping off rain rate may refer unknown properties of much ice crystal and supercooled water in this layer. From the altitude of maximum averaged rain rate to the ground, rain rate is getting less fast

Fig.6. Mean profiles of the eight thermal convective clouds.

possibly induced by broken and evaporating processes of rain droplets during their dropping, which needs to be validated by experimental method.

To better know the rain profile in the meso-β-scale TCS, we compare it with that in a heavy meso-scale convective system (MCS) happened near Wuhan city on July 20, 1998. The rain profiles normalized by rain rate at 2 km for both different convective systems show the same altitude of the maximum averaged rain rate and depth of mixture layer for both systems (see Fig. 7). But the most TCS precipitating clouds are deeper than the heavy MCS precipitating clouds. The averaged storm tops of the former are higher than 10 km, such as cloud A, B, D, and E. While the latter's tops are less than 10 km. That implies much more ice particles inside the TCS precipitating clouds, and stronger ascending flows in the TCS precipitating clouds than in the heavy MCS raining clouds. Additionally,

Fig.7. Normalized precipitation profiles of thermal convective clouds (a) and the heavy precipitating clouds in mesoscale convective system of "98.7.20" (b).

profiles in Fig.7 indicate that rain rate dropping off towards ground faster in the TCS than in the heavy MCS means intensive evaporation processes happened above ground surface in the TCS precipitating clouds due to very hot surface.
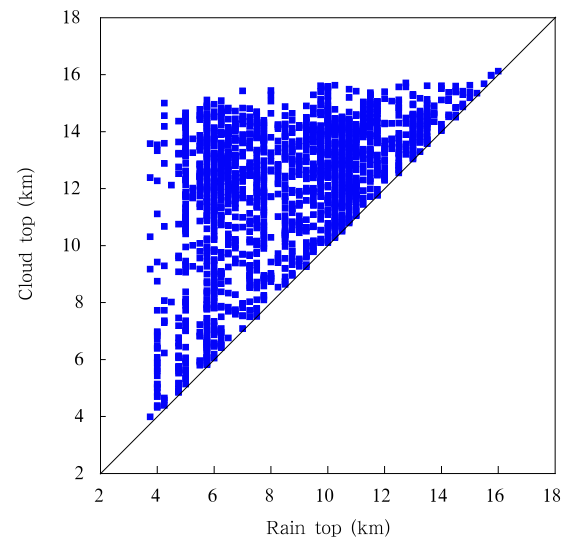
3.4 *Features of the TCS cloud top*

Theoretically, IR temperatures radiated from cloud top image temperatures of the cloud top. In this meaning, the IR temperatures are also determined by the height of the cloud top. Usually, the lower IR temperatures are, the higher cloud top, i.e., the deeper the cloud, and of course, the greater chances of rainfall for the cloud. But, physically, there is no one-to-one corresponding relationship between IR temperature and surface rain rate, which has been illustrated in Fig. 1 that there is only small part of precipitating clouds among clouds. However, we exactly know less about how much proportion of rain clouds in total clouds.

The IR temperature of eight TCS precipitating clouds listed in Table 2 shows that it spreads within 254-286, 204-270, and 202-268 K for channel 3.75, 10.80, and 12.00 μm, respectively. It is clear that the higher the cloud top is, the lower IR temperature radiated from the cloud top is. To clear up relationship among cloud top, storm top, and surface rain rate in the TCS precipitating clouds, we calculate the three parameters at an unified resolution, i.e., TRMM PR resolution 4.3 km, through matching measurements between TRMM PR and IR channels. Results reasonably display that the altitude of cloud top is higher or at least equal to the height of storm top, and a relatively large amplitude variation of cloud tops with lower storm tops, for example, cloud tops vary from 5 km to 15 km corresponding to 5 km storm top (see Fig. 8). While the higher the storm top is, the more consistent is for both cloud top and storm top, which also reflects one of natures for the complicated dynamics and microphysics inside the TCS precipitating clouds.
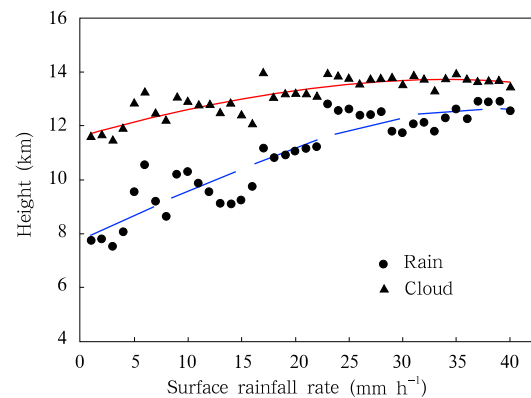
The averaged relationship among cloud top, storm top, and surface rain rate in the TCS precipitating clouds is plotted in Fig.9. It exposes that the larger the surface rain rate, the higher and more con-

sistent both cloud top and storm topure. Basically, the cloud top is 1-4 km higher than storm top for a given surface rain rate, for instance, the cloud top is 4 km higher than storm top in average as 1 mm h^{-1} surface rain rate, and 1 km higher when surface rain rate is 40 mm h^{-1}. The above relationship is needed to be identified by statistics.
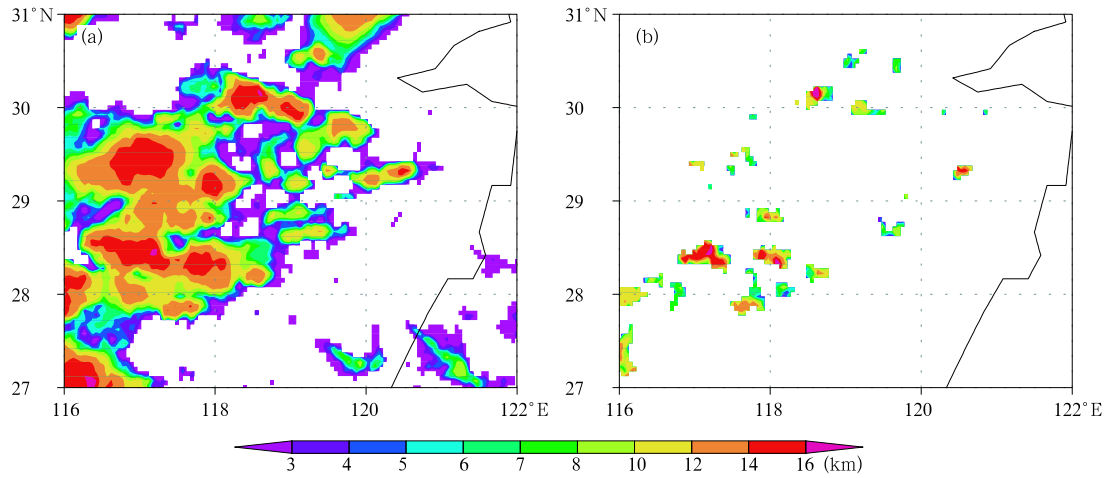
The distribution of the cloud top and storm top shown in Fig.10a indicates that the clouds of the TCS in the WSPA have higher cloud top, most of them over 10 km. While in Fig.10b, it shows that the tops of the

Fig.8. Scattering points of rain-top corresponding to cloud-top at each precipitating pixel in the thermal convective rains.

Fig.9. Relationship of both mean cloud top and mean storm top to near surface rain rate averaged from precipitation pixels.

Fig.10. Distributions of cloud tops (a) and storm tops (b).

scattering precipitating clouds are above 5 km. Moreover, less clear sky exists among these clouds possibly caused by descending compensation flow inside strong convective ascending air. Compared with Figs.1c and 1d, it is easy to find detailed loses in cloud edges in Fig.10 due to the IR resolution having been changed into the PR resolution by unified and matching both IR and PR data.

The statistics of non-precipitating clouds, precipitating clouds, and clear sky in the region 26°-31°N, 115°-119°E is listed in Table 3. For convenience, we simply define three cloud types according to IR temperatures. The high cloud is defined as its IR temperature less than 250 K. If cloud IR temperature is between 250 and 270 K, the cloud is named as the moderate cloud, and the lower cloud's IR temperature

is between 270 and 300 K. As IR temperature is greater than 300 K, the temperature represents clear sky condition. The statistics indicates that there are 85.9% for non-precipitating clouds in the region. Among them, the high, moderate, and lower cloud are 45.8%, 13.1%, and 27.0%, respectively. The coverage of clear sky is only 2.2%. Among 11.9% of precipitating cloud, 2.9%, 5.9%, and 3.1% is for heavy rain cloud (i.e., surface rain rate greater than 10 mm h^{-1}), moderate rain cloud (surface rain rate between and 10 mm h^{-1}), and light rain cloud (surface rain rate less than 1 mm h^{-1}), respectively. Thus it can be seen that the coverage of the TCS precipitating clouds in the WSPA is only a small part in the TCS. But the non-precipitating clouds in the TCS cover a large area that is eight times as that of precipitating clouds.

Table 3. Area fractions of non-precipitating clouds, precipitating clouds, clear sky to the region of 26°-31°N, 115°-119°E

Rain cloud	3.1% (RR<1.0)	5.9% (1.0<RR<10.0)	2.9% (10.0<RR)
High cloud	45.8 % (TBB<250 K)		
Moderate cloud	13.1 % (250<TBB<270 K)		
Lower cloud	27.0 % (270<TBB<300 K)		
Clear sky	2.2 % (300<TBB)		

4. Conclusions

In this paper, standard TRMM products derived from measurements of TRMM PR and IR are used to analyze characteristics of precipitating clouds in a thermal convective system (TCS) occurred in the

southeastern mainland of China at 15:00 BT on August 2, 2003 in the central western subtropical pacific anticyclone (WSPA). The goal of this study is to learn natures of precipitating clouds in the TCS inside the central WSPA through their rain profiles, IR temperatures, which will be helpful for understanding

properties of both the TCS and the WSPA, and supply as a true counterpart for simulation validations.

Results indicate these isolated precipitating clouds of the TCS are situated within the central WSPA at 500 hPa and the central convergent depression at 1000 hPa. Seven hours (i.e., 8:00 BT) before the TCS occurring, sounding profiles near the TCS region show dry and no instable energy below the middle atmosphere but convection instability state exists in atmosphere at that moment. In the phase 2 h before the TCS happens, records in surface chart show that near surface temperatures are over $39°C$, even exceeding $40°C$, observed by most weather stations near the TCS region. Records also indicate relatively dry air near surface before TCS occurs. But, the four-time daily NCEP/NCAR reanalysis data displays that strong ascending flows at 500 hPa and strong convergence of moisture fluxes at 850 hPa in the center of the WSPA at 1 h before the TCS happening supply necessary conditions both in dynamics and moisture for the TCS development.

The TRMM PR observation shows that the horizontal scale of precipitating clouds varies from 10 to 80 km, but most of them are 30-40 km meso-β-scale in the TCS. The maximum rain rate near surface of those TCS clouds is beyond 50 mm h^{-1}. Their averaged vertical scale is above 10 km, the maximum reaches 17.5 km that is above the top of the troposphere. The mean rain profile of the TCS clouds shows its maximum rain rate at 5-km altitude that is 1 km lower than the estimated freezing level of the environment. Compared with the mesoscale convective system (MCS) of "98.7.20", both systems have the same altitude of the maximum rain rate displayed from both mean rain profiles. But the TCS is much deeper than the MCS. The averaged storm tops of the TCS are higher than 10 km contrary to less than 10 km for the MCS. From the altitude of the maximum rain rate to near surface, profiles show that rain rate reducing in the TCS is faster than that in the MCS, which implies a strong droplet evaporation process occurring in the TCS.

Features of cloud top derived from PR and IR observations show that a large variation of cloud top when storm top is lower, for example, cloud tops vary from 5 to 15 km corresponding to 5 km storm top. On the contrary, the higher the storm top is, the more consistent both the cloud top and storm top are. The relationship among cloud top, storm top, and surface rain rate in the TCS precipitating clouds shows that the larger the surface rain rate is, the higher and more consistent both the cloud top and storm top are. In average, cloud-top is 1-4 km higher than storm-top for a given surface rain rate. The statistics of non-precipitating clouds, precipitating clouds and clear sky expose that area fractions of non-precipitating clouds and clear sky are 86% and 2%, respectively. Among the non-precipitating clouds, the high, moderate, and lower cloud are 45.8%, 13.1%, and 27.0%, respectively. The area fraction of precipitating clouds is near 12% that is about 1/8 that of non -precipitating clouds.

REFERENCES

Awaka, J., T. Iguchi, and K. Okamot, 1998: Early results on rain type classification by the Tropical Rainfall Measuring Mission (TRMM) precipitation radar. Pro. 8th URSI commission F Open Symp. Averior, Portugal, 134-146.

Cui Chunguang, Min Airong, and Hu Bowei, 2002: Dynamic effect of mesoscale terrain on "98.7" extremely heavy rain in the east of Hubei Province. *Acta Meteorologica Sinica*, **60**(5), 602-612.(in Chinese)

Ding Yihui, 1993: A *Study of the Prolonged Heavy Rainfall in the Yangtze-Huaihe River Basins in 1991.* China Meteor Press, Beijing, 255pp (in Chinese).

Fu Y., Liu G., and Lin Y., 2002: Rainfall in Tibet Plateau as viewed by TRMM satellite. TRMM International Science Conference, 22-26 July, Honolulu, Hawaii, p72.

Fu Y., and Liu G., 2003: Precipitation characteristics in mid-latitude East Asia as observed by TRMM PR and TMI. *J. Meteor. Soc. Japan*, **81**, 1353-1369.

Fu Y., Lin Y., Liu G., et al, 2003a: Seasonal characteristics of precipitation in 1998 Over East Asia as derived form TRMM PR. *Adv. Atmos. Sci,* **20**, 511-529.

Fu Yunfei, Yu Rucong, Xu Youping, et al., 2003b:

Analysis on precipitation structures of two heavy rain cases by using TRMM PR and TMI. *Acta Meteorologica* Sinica, **61**(4), 421-431. (in Chinese)

Fu Y., Li R., Liu G., et al., 2004: Characteristics of precipitation clouds over Asia during summer as derived from TRMM PR and TMI, 14th International Conference on Clouds and Precipitation. 19-23 July, 2004, Bologna, Italy, 1646-1649.

Fu Y., and Liu G., 2001: The variability of tropical precipitation profiles and its impact on microwave brightness temperatures as inferred from TRMM data. *J. Appl. Meteor.*, **40**, 2130-2143

Guo Qiyun, 1985: The variations of summer monsoon in East Asia and the rainfall over China. *Journal of Tropical Meteorology*, **1**(1), 44-52. (in Chinese)

Huang Ronghui and Li Weijing, 1988: The effect of heat source anomaly over the tropical western Pacific during summer. *Chinese J. Atmos. Sci.*, **12** (Special issue), 107-116. (in Chinese)

Houze, R. A. Jr., 1997: Stratiform Precipitation in Regions of Convection: A Meteorological Paradox? *Bull. Amer. Meteor. Soc.*, **70**: 282-285.

Iguchi, T., and R. Meneghini, 1994: Intercomparison of single-frequency methods for retrieving a vertical rain profile from airborne or spaceborne radar data. *J. Atmos. Oceanic Technol.*, **11**, 1507-1516.

Kummerow, C., W. Barnes, et al., 1998: The Tropical Rainfall Measuring Mission (TRMM) Sensor Package. *J. Atmos. and Ocean Tech.*, **15**, 809-817.

Lu Weisong, Wang Qinliang, and Peng Yongqing, 1995: Nonlinear Critical Layer and Generation of Subtropical *High. Scientia Atmospherica Sinica*, **19**(1), 37-81. (in Chinese)

Wang Xiaochun and Wu Guoxiong, 1997: The Analysis of the Relationship between the Spatial Modes of Summer Precipitation Anomalies over China and the General Circulation. *Scientia Atmospherica Sinica*, **21**(2), 161-169. (in Chinese)

Liu Yimin, Wu Guoxiong, Liu Hui, et al., 1999: The effect of spatially nonuniform heating on the formation and variati on of subtropical high part III:Condensation heating and south Asia high and Western Pacific subtropical high. *Acta Meteorologica Sinica* **57**(5), 525-538. (in Chinese)

Liu Yimin and Wu Guoxiong, 2000: Reviews on the study of the subtropical anticyclone and new insights on some fundamental problems. *Acta Meteorologica Sinica*, **58**(4), 500-512. (in Chinese)

Liu G., and Fu Y., 2001: The characteristics of tropical precipitation profiles as inferred from satellite radar measurements. *J. Meteor. Soc. Japan*, **79**, 131-143.

Li Rui, Fu Yunfei, and Zhao Ping, 2005: Characteristics of rainfall structure over the tropical Pacific during the later period of 1997/1998 El Nino derived from TRMM PR observations. *Chinese Journal of Atmospheric Science.* **29**(2), 225-235. (in Chinese)

Sun Jian, Zhao Ping, and Zhou Xiuji, 2002: The mesoscale structure of a South China rainstorm and the influence of complex topography. *Acta Meteorologica Sinica*, **60**(3), 333-341. (in Chinese)

Simpson, J., R. F. Adler, and G. R. North, 1988: A proposed tropical rainfall measuring mission (TRMM) satellite. *Bull. Amer. Meteor. Soc.*, **69**, 278-295.

Tao Shiyan and Zhu Fukang, 1964: The 100mb Flow Patterns in Southern Asia in Summer and Its Relation to the Advance and Retreat of the West-Pacific Subtropical Anticyclone over the Far East. *Acta Meteorologica Sinica*, **34**(4), 385-395. (in Chinese)

Tao Shiyan, Ding Yihui, and Zhou Xiaoping, 1979: The present status of the research on rainstorm and severe convective weathers in China. *Scientia Atmospherica Sinica*, **3**(3), 227-238. (in Chinese)

Tao Shiyan et al., 1980: *Torrential Rain in China*. Science Press, Beijing, 225pp. (in Chinese)

Tao W-K, J. Simpson, and R. F. Adler, 1993: Retrieval algorithms for estimating the vertical profiles of latent heat release: Their applications for TRMM. *J. Meteor. Soc. Japan*, **71**, 685-700.

Wu Guoxiong, Chou Jifan, Liu Yimin, et al., 2000: *Dynamics of the formation and variation of subtropical anticyclones*. Science Press, Beijing, 314pp. (in Chinese)

Yu Shihua and Zhao Ku, 1993: The comparative analysis of the anomanously advancing and retreating of subtropical High in western Pacific ocean. *Journal of Tropical Meteorology*, **9**(1), 12-19. (in Chinese)

Zhao Hanguang and Zhang Xiangong, 1996: The Relationship between the summer rain belt in China and the East Asia Monsoon. *Meteorlogical Monthly*, **22**, 8-12. (in Chinese)

Zhang Qingyun and Tao Shiyan, 1998: Tropical and subtropical monsoon over East Asia and its influence on the rainfall over eastern China in summer. *Quarterly Journal of Applied Meteorlogy*, **9** (supplement), 16-23. (in Chinese)

Zheng Yuanyuan, Fu Yunfei, Liu Yong, et al., 2004: Heavy rainfall structures and lightning activities in a cold front cyclone happened in huaihe River derived from TRMM PR and LIS observations. *Acta Meteorologica Sinica*, **62**(6), 790-802. (in Chinese)